Pure appl. geophys. 159 (2002) 1021–1041
0033–4553/02/051021–21 $ 1.50 + 0.20/0

Pure and Applied Geophysics

Adaptive Training of Neural Networks for Automatic Seismic Phase Identification

JIN WANG[1]

Abstract—A neural network module has been implemented in the Prototype International Data Centre (PIDC) for automated identification of the initial phase type of seismic detections. Initial training of the neural networks for stations of the International Monitoring System (IMS) requires considerable effort. While there are many seismic phases in the analyst-reviewed database that can be assumed as the ground-truth resource of the initial phase type of Teleseism (T), Regional P (P), and Regional S (S), no ground-truth database of noise (N) is available. To reduce analyst effort required in building a ground-truth database, an "Adaptive Training Approach" is proposed in this paper. This approach automatically selects training patterns to take advantage of the learning ability of neural networks and information on the accumulated observation database. Using this approach, neural networks were trained on the data provided by station STKA, Australia. The performance of automated phase identification has been improved significantly by the retrained neural networks. This approach is also validated by comparison with the performance using the ground-truth noise database.

Key words: Artificial Intelligence, Neural Networks, CTBT, Seismic Phase Identification.

1. Introduction

Phase identification is a major task in operating an automated seismic monitoring system. The accuracy of the phase identification significantly impacts the final automated bulletin. The availability of digital three-component seismograms improves the chance of automatically identifying the *P*- and *S*-phase arrivals of seismic events. A number of algorithms have been developed to automatically identify seismic phase type, and research continues in improving the reliability of these algorithms and in reducing the overhead time. For example, JURKEVICS (1988) presented a technique for polarization analysis of three-component seismic data. ROBERTS *et al.* (1989) presented a technique for phase identification based on the auto- and cross-correlations of the three-component seismic data. BACHE *et al.* (1990) developed the first operational version of the

[1] Center for Monitoring Research, Science Applications International Corporation, 1300 N. 17th Street, Suite 1450, Arlington, VA 22209, U.S.A. E-mail: wangjin2000@yahoo.com

Intelligent Monitoring System, which now has been employed as the Prototype International Data Centre (PIDC) in Arlington, Virginia, USA, and as the International Data Centre for the Comprehensive Nuclear-Test-Ban Treaty Organization in Vienna, Austria. A rule-based expert system for initial phase identification was applied in that system. SUTEAU-HENSON (1991) presented a study on phase identification based on polarization analysis for three-component data. SERENO and PATNAIK (1993) developed a neural network module for automated identification of the initial phase type of seismic detections and implemented that module at the PIDC. CICHOWICZ (1993) developed an algorithm for automatically picking the *S* phase from three-component seismograms. WANG and TENG (1995, 1997) designed two artificial neural network based detectors for picking and identifying regional *P* and *S* phases. ANANT and DOWLA (1997) applied wavelet transform methods to phase identification for three-component seismograms.

While most of these examples have not been tested extensively in the operational environment, the neural network module developed by SERENO and PATNAIK (1993) has been implemented in the PIDC operational system since 1995. In the initial implementation, a set of average weights trained from a limited number of stations was used as a set of default weights for three-component stations. All detections at three-component stations were automatically classified into different phase types by the neural networks in routine operations. Like any other automatic monitoring system, the automatic network solutions were reviewed, and corrected if necessary, by skilled human analysts to generate final solutions. The corrections by analysts include changing signal onset time, changing assigned phase identifier, or changing which detections were grouped together and associated with a single seismic event. The reviewed results were called the "analyst reviewed bulletin" in the PIDC. Evaluations of phase identification with the default weights at the PIDC showed that the performance varies at different stations. The correct rate of the initial phase-type identification in the automated event bulletin compared to the analyst reviewed database ranged from 25.6% to 73.4%. The PIDC has accumulated millions of seismic phase readings for the current three-component stations, which were not available at the time of the original neural network implementation. Therefore, it is worthwhile to train neural networks for each specific station to improve the performance of automatic phase identification, which, in turn, will improve the quality of the automatic event bulletin. Although many seismic phases that were reviewed by analysts in the PIDC database can be assumed to be the ground-truth resource, no ground-truth database of noise is available. This is a major obstacle for updating the neural networks. This paper proposes an approach to training neural networks that takes advantage of accumulated seismic phases and the adaptive learning ability of neural networks.

2. Artificial Neural Networks

Artificial neural networks are inspired by biological systems in which large numbers of neurons, which individually function rather slowly and imperfectly, collectively perform tasks that even the fastest computers have not been able to match. This field is among the most rapidly developing scientific research today and is interdisciplinary in nature. Its potential applications include speech and image recognition, linear and nonlinear optimization, automatic control, and seismology.

As in a biological nervous system, fundamental elements of an artificial neural network are artificial neurons (also called cells, units, or nodes). The function of artificial neurons is identical to that of real neurons: they integrate input from other neurons and communicate the integrated signal to a decision making center. Computational models of a neural network try to emulate the physiology of real neurons. Artificial neural networks have two principal functions: one is the input-output mapping or feature extraction. The other is the pattern association or generalization. The mapping of input and output patterns is estimated or "learned" by neural networks with representative samples of the input and output pattern (training set). The generalization of neural networks is an output pattern in response to an input pattern, based on the neural network memories that were learned in the training process.

Among many different types of neural networks, a particular type, the Multi-Layered Perceptron (MLP), is used in the routine operation in the PIDC. A perceptron may be viewed as a neuron that computes activation with a sigmoidal activation function, which takes the following form (ZURADA, 1992):

$$o_i = F(d_i) = \frac{1}{1 + \exp(-\beta d_i)}$$

where

$$d_i = \sum_{i}^{N} w_{ij} x_j - \theta_i \ ,$$

where o_i is the activity output at neuron i, constant β controls the slope of the semi-linear region, d_i is the weighted sum of neuron i for the input from the last lower layer with N neurons, x_j is the input from neuron j, w_{ij} is the weight between neurons i and j, and θ_i is the intrinsic threshold that can be treated as an individual weight with a negative sign.

The structure of an artificial neuron is shown in Figure 1. The one-to-one correspondence between an artificial neuron and a biological neuron is commonly drawn: the inputs correspond to the dendrites of a biological neuron; the weights correspond to the synapses; the summation and the transfer function correspond to the cell body; and the output to other neurons corresponds to axons. Artificial neural

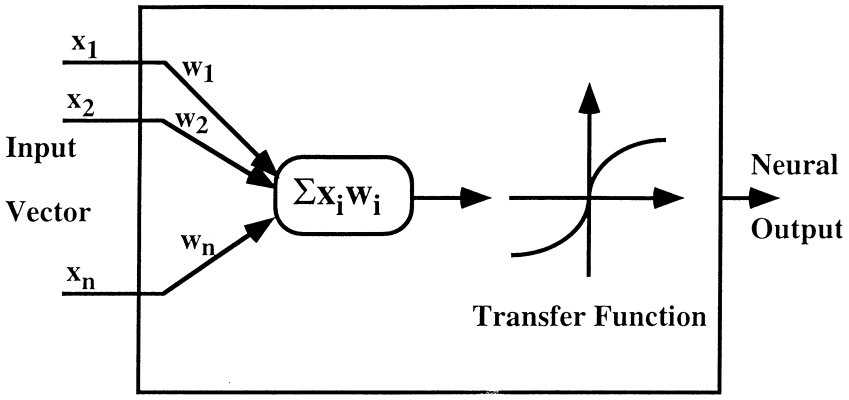

Figure 1
Architecture of single artificial neuron consisting of N input units. The input vector fans in from the left and fans out to the right. Interconnection of artificial neurons forms a complex architecture called an artificial neural network.

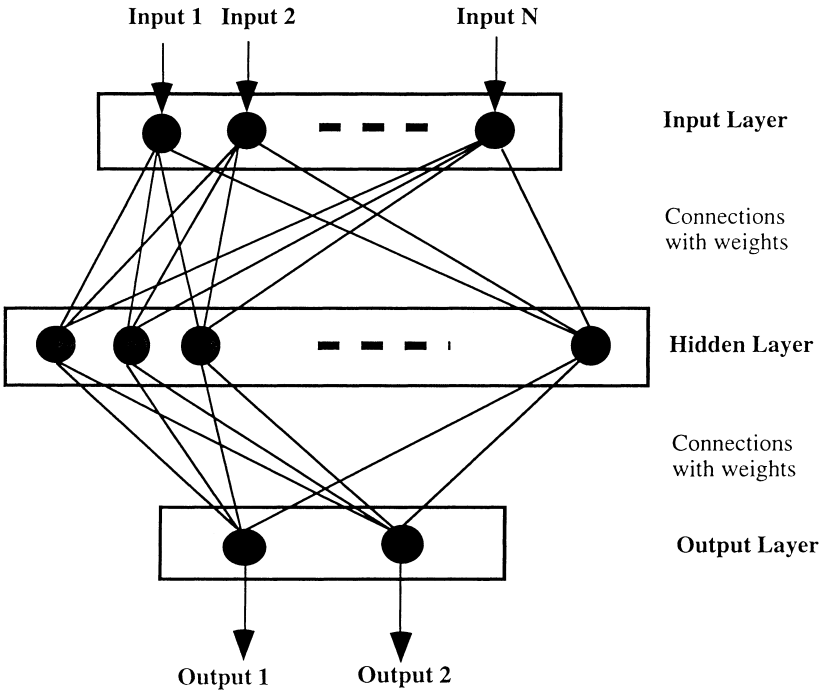

Figure 2
Structure of multi-layered perceptron neural network. It is a feedforward and partially connected network. Neurons are only connected to the adjacent layer neurons.

networks can be constructed by linking the neurons through the weights. A multi-layer feed-forward network is shown in Figure 2. The input data are propagated or feedforwarded through neurons and their connections in the hidden layer to the output neurons.

The weights of a neural network are obtained by learning through the training data set. The most widely used algorithm for a multi-layer feedforward neural network is the backward error propagation algorithm for supervised learning (RUMELHART *et al.*, 1986). An objective function in the output layer is defined by

$$J_p = \frac{1}{2M}\sum_{k=1}^{M}[T_k(p) - O_k(p)]^2 \ ,$$

and the normalized sum of objective function over total training set is defined by

$$J = \frac{1}{p}\sum_{p=1}^{p} J_p \ ,$$

where M is the number of outputs of the neural network, $T_k(p)$ is the desired (or called target) output of the k-th neuron for the training pattern p, and $O_k(p)$ is the actual neural output of the k-th neuron. The back propagation learning algorithm uses a least-squares error minimization criterion to minimize J by adjusting the weights. That is, the learning process is supervised by the given input-output pattern set, and it will end if the J has converged to a desired value.

The trained neural network will be used to process and classify unknown input data. Successful application of the neural networks for pattern recognition is highly dependent on the training process. For supervised learning, the performance of a trained neural network is related to the quality of the selected training patterns.

3. Automatic Phase Identification at the PIDC

Phase identification is a major task in operating an automated seismic monitoring system. In the PIDC software system, signals detected in seismic stations first are categorized as one of four initial wave types: noise (*N*), teleseismic waves (*T*), regional *P* wave (*P*), or regional *S* wave (*S*). Signals are characterized based on their features and qualities extracted from the waveforms near the arrival time. For detections from three-component stations, a neural network is applied to determine the initial wave type.

In the software developed by Science International Applications Corporation (SAIC), the four initial wave-type classification problem is solved by three cascaded neural networks of the MLP (SERENO and PATNAIK, 1993). Each of the three neural networks consists of three layers: an input layer, a hidden layer, and an output layer. The input layer consists of 15 nodes, corresponding to 15 features; the hidden layer

consists of 6 nodes, and the output layer consists of two nodes that correspond to the two output classes. The first neural network distinguishes between noise and signal, the second distinguishes between teleseismic and regional phases, and the last determines if the regional phases are *P* or *S*. The three types of initial phase (*T*, *P*, *S*) are further divided into final phases such as *P*, *PKP*, *Pn*, *Pg*, *Sn*, and *Lg* by other subprograms, and are used for automatic event formation and phase association. The noise detections, however, are not further processed by automatic operations.

The 15 attributes used for the input of each of the three neural networks include dominant period, polarization attributes, contextual attributes, and a spectral representation of the horizontal-to-vertical power ratio. Polarization is the main source of information, which can be derived from three-component seismic data. The method used for polarization analysis was developed by JURKEVICS (1988), and its implementation in the IMS was described by BACHE *et al.* (1990).

For polarization measurement, the convariance matrix of three-component seismic data, *S*, is evaluated by:

$$S_{jk} = \frac{1}{N}\sum_{i=1}^{N} x_{ij}x_{ik} \quad ,$$

where x_{ij}, x_{ik} are the waveform data in a time window, i is the index of the sample in the time window, N is the number of samples, and j or k is the index of the component (z, n, e).

The terms of the 3×3 convariance matrix are the auto- and cross-variances of the three components of the ground motion:

$$S = \begin{bmatrix} s_{zz} & s_{nz} & s_{ez} \\ s_{zn} & s_{nn} & s_{en} \\ s_{ze} & s_{ne} & s_{ee} \end{bmatrix} \quad .$$

The polarization ellipsoid is computed by solving the eigenvalue problem for the covariance matrix, which yields the eigenvalues $(\lambda_1, \lambda_2, \lambda_3)$ and eigenvectors $(\boldsymbol{u}_1, \boldsymbol{u}_2, \boldsymbol{u}_3)$ of the matrix.

Feature extraction (attribute selection) and pattern classification are two basic steps for a pattern recognition. The two steps are closely related; a better feature extraction will result in an easier classification. The success of a neural work system for pattern classification primarily depends on the designer's physical understanding of the problem. Fifteen attributes used in the neural networks for initial wave-type classification are based on previous studies and are proven successful (SERENO and PATNAIK, 1993). Other different feature combinations that have better performance might be found by further research. However, that discussion is beyond the scope of this paper. The goal of this paper is to tune the neural networks under the same structure that has been used for the PIDC. The following 15 attributes are used in the neural networks:

(1) *period*: Dominant period of the detected phase.
(2) *rect*: Signal rectilinearity: $rect = 1 - \frac{\lambda_2+\lambda_3}{2\lambda_1}$, where $\lambda_1 > \lambda_2 > \lambda_3$ are eigenvalues obtained by solving the 3-D eigensystem.
(3) *plans*: Signal planarity: $plans = 1 - \frac{2\lambda_3}{\lambda_1+\lambda_2}$, which is a measure of the planar characteristic of the polarization ellipsoid.
(4) *inang1*: Long-axis incidence angle: $inang1 = \frac{a\cos(|u_{11}|)}{90}$, where *inang*1 is a normalized angle measured clockwise from the vertical axis, and u_{11} is the direction cosine of the eigenvector associated with the largest eigenvalue.
(5) *inang3*: Short-axis incidence angle: $inang3 = \frac{a\cos(|u_{31}|)}{90}$, where *inang*3 is a normalized angle measured clockwise from the vertical axis, and u_{31} is the direction cosine of the eigenvector associated with the smallest eigenvalue.
(6) *hmxmn*: Ratio of the maximum to minimum horizontal amplitude: $hmxmn = \sqrt{\frac{\lambda_1}{\lambda_2}}$, where λ_1 and λ_2 are the maximum and minimum eigenvalues obtained by solving the 2-D eigensystem using only the horizontal components.
(7) *hvratp*: Ratio of horizontal-to-vertical power: $hvratp = \frac{s_{nn}+s_{ee}}{2s_{zz}}$, where s_{zz}, s_{nn}, and s_{ee} are the diagonal elements of the covariance matrix measured at the time of maximum rectilinearity.
(8) *hvrat*: Similar to *hvratp*, however measured at the time of the maximum three-component amplitude.
(9) $N_{\text{after}} - N_{\text{before}}$: Difference between the number of arrivals before and after the arrival in question within a fixed time window (60 seconds by default). The value of the number difference is scaled to a small range near ± 1 by dividing by 10.
(10) $T_{\text{after}} - T_{\text{before}}$: Mean-time difference between the arrival in question and those arrivals before and after it within a fixed time window (60 seconds by default). The value of the mean time difference is scaled to a small range near ± 1 by dividing by 100.
(11) *htov1*: Horizontal-to-vertical power ratio in an octave frequency band centered at 0.25 Hz.
(12) *htov2*: Horizontal-to-vertical power ratio in an octave frequency band centered at 0.5 Hz.
(13) *htov3*: Horizontal-to-vertical power ratio in an octave frequency band centered at 1.0 Hz.
(14) *htov4*: Horizontal-to-vertical power ratio in an octave frequency band centered at 2.0 Hz.
(15) *htov5*: Horizontal-to-vertical power ratio in an octave frequency band centered at 4.0 Hz.

This paper uses the three-component station STKA, which is located at Stephens Creek, Australia (31.88 S, 141.60 E), as a demonstration station. Figures 3–5 show histograms of the 15 attributes for the selected *T*-, *P*-, *S*- and *N*-type phases for station STKA from January 1 to October 26, 1996. In Figure 3, the distribution of signal periods for the four types is similar; the rectilinearity distributions can be

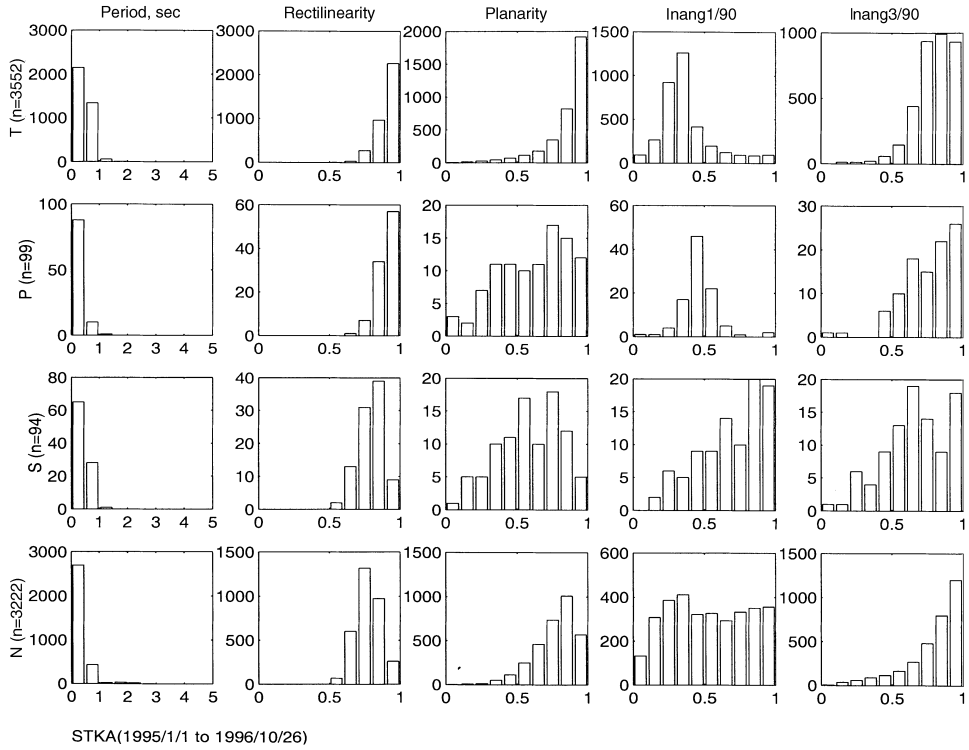

Figure 3

Histograms of period, rectilinearity, planarity, long-axis incidence angle and short-axis incidence angle grouped by four initial wave types for station STKA. The distribution of signal periods for the four types are almost the same; the rectilinearity distributions can be divided into two groups, one for teleseismic and regional *P* phases (*T* and *P*), and one for regional *S* wave and noise (*S* and *N*); the planarity distributions are different for each type, and *Inang*1 distributions are also different for each type; the *Inang*3 distributions are similar for the *T* and *P* types, but are distinguished for the *S* and *N* types.

divided into two groups; one for teleseismic and regional *P* phases (*T* and *P*), and one for regional *S* wave and noise (*S* and *N*); the planarity distributions are different for each type, and the *Inang*1 are also different for each type; the *Inang*3 distribution is similar for the *T* and *P* types, but is different for the *S* and *N* types. In Figure 4, the five attribute distributions are quite different but exhibit some overlapping. In Figure 5, the horizontal-to-vertical power ratios in five frequency bands show some differences although with no significance. Therefore, the 15 attribute distributions in Figures 3–5 demonstrate considerable overlapping among the four initial phase types. Neural networks are well-suited for this condition because they are capable of constructing nonlinear decision surfaces across complex class boundaries from high-dimensional input data.

As the initial implementation, a set of average weights trained from a limited number of stations was used as a set of default weights for three-component stations

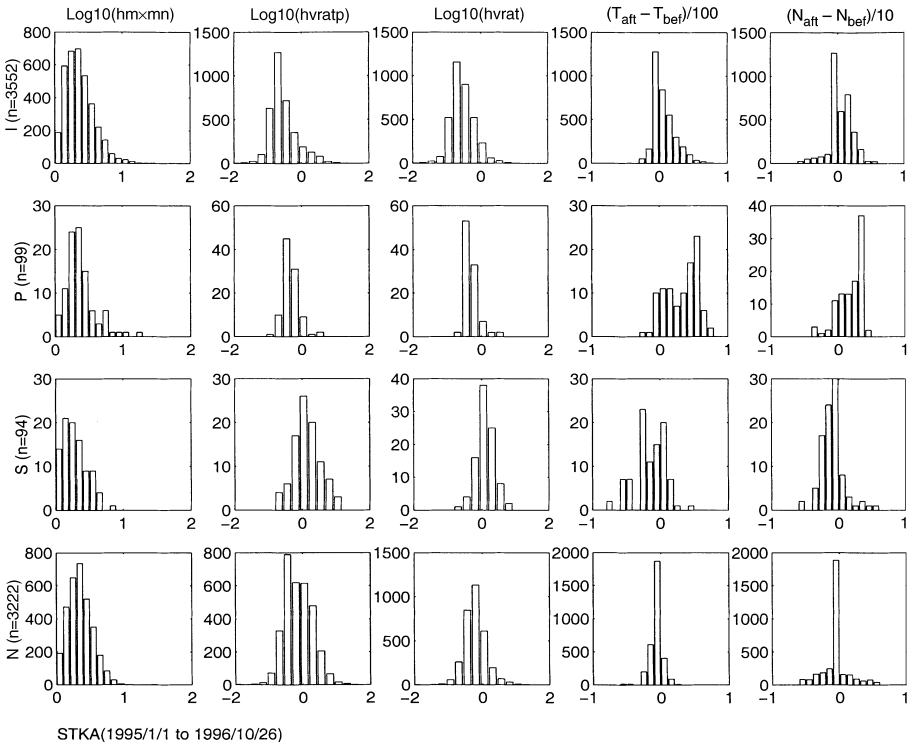

Figure 4

Histograms of maximum-to-minimum horizontal amplitude ratio, horizontal-to-vertical power ratio at the time of maximum rectilinearity and at the time of maximum three-component amplitude, the difference of arrival times (($T_{aft} - T_{bef}$)/100) and detection numbers (($N_{aft} - N_{bef}$)/10) between that after and before the detection in question within a fixed time window of 60 seconds grouped by four initial wave types for station STKA. In the figure, five attribute distributions are quite different but have some overlapping.

in the PIDC. To evaluate how well the default weights performed for the automatic initial wave-type identification, the initial wave type of detections in the automatic bulletin was compared to those in the final analyst reviewed bulletin for station STKA. Table 1 indicates a "confusion matrix" of initial wave types from July 11 to November 25, 1996. The matrix indicates how the phase types classified by the neural networks were finally classified by analysts. Each row in the table is the number of initial wave types determined by the automatic system, and each column is the number of the types confirmed by analysts. Ideal performance of the automated system should result in zero for off-diagonal elements of the matrix. The "correct rate" is defined as the ratio of the sum of the diagonal elements to the total number of the phases in the final analyst reviewed bulletin; for STKA it was $704/2755 * 100\% = 25.6\%$. Table 1 shows that many teleseismic phases in the final analyst reviewed bulletin were incorrectly identified as regional *P*-type phases in the automatic bulletin. In addition, 22.8% (629/2755) of phases in the final analyst

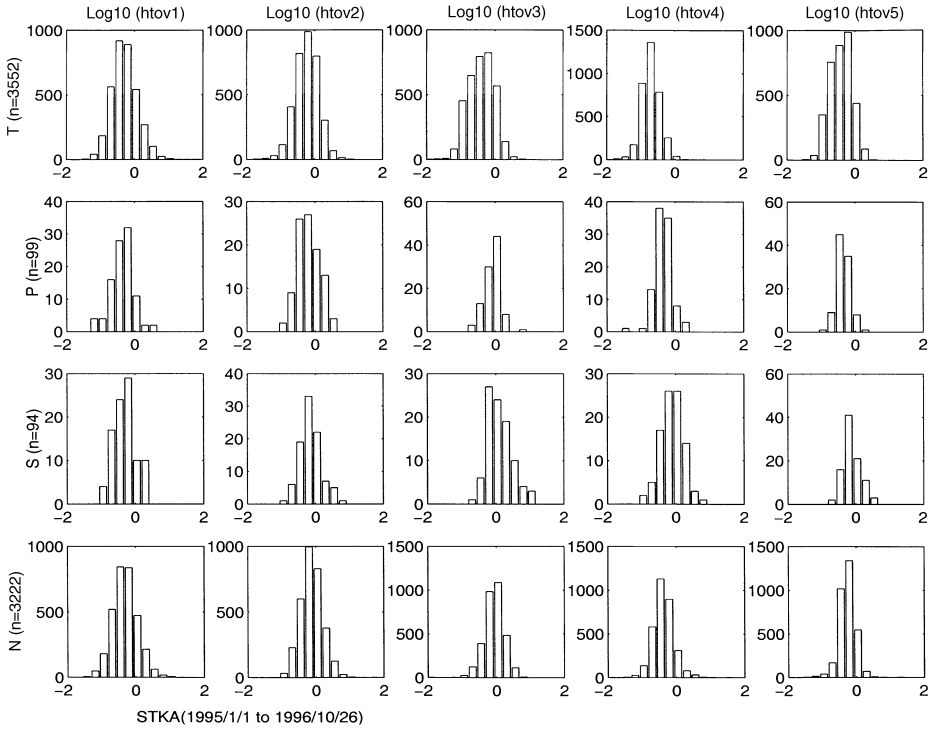

Figure 5
Histograms of horizontal-to-vertical power ratio at center frequencies of 0.25, 0.5, 1.0, 2.0, and 4.0 Hz grouped by four initial wave types for station STKA. They show some differences but with no significance.

Table 1

Confusion matrix of initial phase classification for STKA using default weights of neural networks (1996/07/19–1996/11/25). Each row in the table is the result by the automatic system, and each column is the final result confirmed by analysts. Off-diagonal elements are misclassification numbers

		Results by analyst			Sum
		T	*P*	*S*	
Results by system	*T*	681	3	0	684
	P	1381	14	3	1398
	S	35	0	9	44
	N	626	1	2	629
	Sum	2723	18	14	2755

reviewed bulletin were incorrectly identified as *N*-type phases in the automatic bulletin. This percentage, defined as the "*N*-phase rate", is another measure of the automatic system's performance. Because the *N* phases in the automatic bulletin would not be associated to form and locate events by the automatic system, reducing

the number of *N* phases that must be renamed and associated in the final analyst bulletin would reduce the work load of analysts.

4. Adaptive Training Procedure for Neural Networks

The evaluation described in the previous section shows that the initial default weights do not work well for station STKA. The neural networks for initial wave-type classification need to be retrained. Selection of a training data set is an important process in the application of neural networks. For supervised learning, the performance of the trained neural networks is related to the quality of the selected training patterns. The initial phase types reviewed by analysts in the analyst reviewed bulletin can be assumed to be accurate (ground truth). This means that many seismic phases are available in the final analyst reviewed bulletin as a ground-truth resource of the initial phase type of *T*, *P*, and *S*. For noise, however, no corresponding ground-truth resource is available. Building a ground-truth database with the help of analysts requires considerable effort. This is a major obstacle for updating the neural networks. This paper proposes a training approach that automatically and adaptively selects training patterns of seismic phases to take advantage of the learning ability of neural networks and information regarding the accumulated operational database. This ''Adaptive Training Approach'' is described in the following sections.

For teleseismic phases (*T*), training samples are randomly selected from the analyst reviewed database, of which the corresponding arrivals have no onset-time corrections between the automatic and the analyst reviewed databases. This restriction ensures that the 15 attributes of signals were calculated accurately from proper time windows.

Because the analyst reviewed database has fewer regional phases, the training samples for regional *P*- and *S*-type phases (*P* and *S*) are selected from the analyst reviewed database for those arrivals with onset-time corrections less than two seconds between the automatic and the analyst reviewed databases. This looser restriction compared with the *T*-type phase selection allows the use of more regional phases at the limited risk of less accurate signal attributes.

Because no ground-truth information is available for noise phases, training samples are randomly selected from *N* phases that were classified to noise detections in the automatic database but were not renamed/associated in the analyst reviewed bulletin. This initial selection assumes that the existing neural network classified the noise detections reasonably well after excluding phases that were renamed by analysts. Most of the selected *N* phases in the initial training set are likely to be true noise detections, although some could be seismic phases that were not associated in the analyst reviewed bulletin.

During the training process, a subset of the selected data is used for the supervised learning. A separate subset of data is used for testing after each training iteration. The comparison between input and output of the trained neural network can be written as a matrix:

	Output Signals	Output Noise
Input Signals	N_{11}	N_{12}
Input Noise	N_{21}	N_{22}

N_{11} is the number of "true" signal detections correctly classified by the neural network; and N_{22} is the number of "true" input noise detections correctly classified. The off-diagonal numbers of the matrix, N_{12} and N_{21}, reflect phase confusion by the trained neural network at each cycle of the training iterations. Ideally, for a training data set, output of the neural network that is being trained would converge to a perfect "correct rate" (100%) after a certain number of iterations. In reality, however, training patterns of two classes may not be selected perfectly correct; the neural network cannot distinguish two classes, therefore the "correct rate" of the neural network output only converges to a percentage value.

As a starting point of training the neural network for classification of signals and noise (stage 1) in this experiment, the noise training patterns were selected from the automatic database under some assumptions. The initial training set of noise phases might be contaminated by unassociated seismic signals, so that the neural network cannot distinguish them from the training patterns of the seismic signals during the training process. The initial training set for station STKA consists of 905 patterns (two thirds of the total), and the testing set consists of 453 patterns (one third of the total). Figure 6 shows the correct rate of training and test results versus the number of iterations for the initial training data set of the station STKA. Correct rates of neural network output converge after about 10,000 iterations: 87% of the training patterns was correctly identified, while 77% of the testing patterns was correctly identified. Specifically, the output of the trained neural network is listed in Table 2. Ninety-four patterns (group N_{21}) in the noise training class were classified to signal class by the trained neural network. Twenty-four patterns (group N_{12}) in the signal training class were classified to noise class by the trained neural network. The confusion matrix for the training result infers that the initial training set had some misclassified patterns.

As an adaptive step, the confused training patterns in group N_{21} were deleted from the initial training set. This group of detections may have similar features with the ground-truth signals and is likely to be unassociated seismic phases. The noise training data set will be purified after this group of detections is removed. The confused training patterns in group N_{12} are still kept as these confusions might be caused by the existence of group N_{21}. The remaining training data is called the

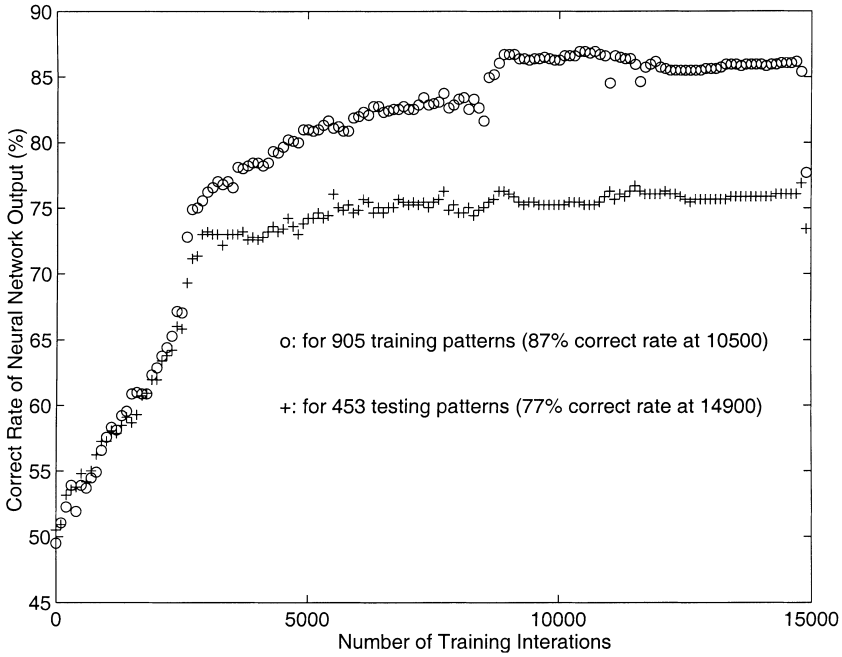

Figure 6
Training and test results of trained neural network (signals versus noise) with initial training set. Output of trained neural network converges after a certain number of learning iterations, and can only correctly classify 87% of the training data set and 77% of the testing data set.

Table 2

Confusion matrix of stage-1 neural network with initial training data set. Each row in the table is the known class of the training data result, and each column is the output of the trained neural network. Off-diagonal elements are misclassification numbers

	Output signal class	Output noise class	Total	Correct rate (%)
Input signal class	428	24	452	94.7
Input noise class	94	359	453	79.2
Total	522	383	905	87.0

"adaptive-1" training data set. In this experiment the size of the training data set is reduced from 905 to 811. The neural network is retrained with the adaptive-1 training set. Figure 7 shows the new results of the neural network for the adaptive-1 training data set. The output of the neural network converges after about 3000 iterations. The correct rate for the training data set increased from 87% to 99% in the initial training step. The neural network must classify training patterns correctly after the learning process. More importantly, the trained neural network can classify

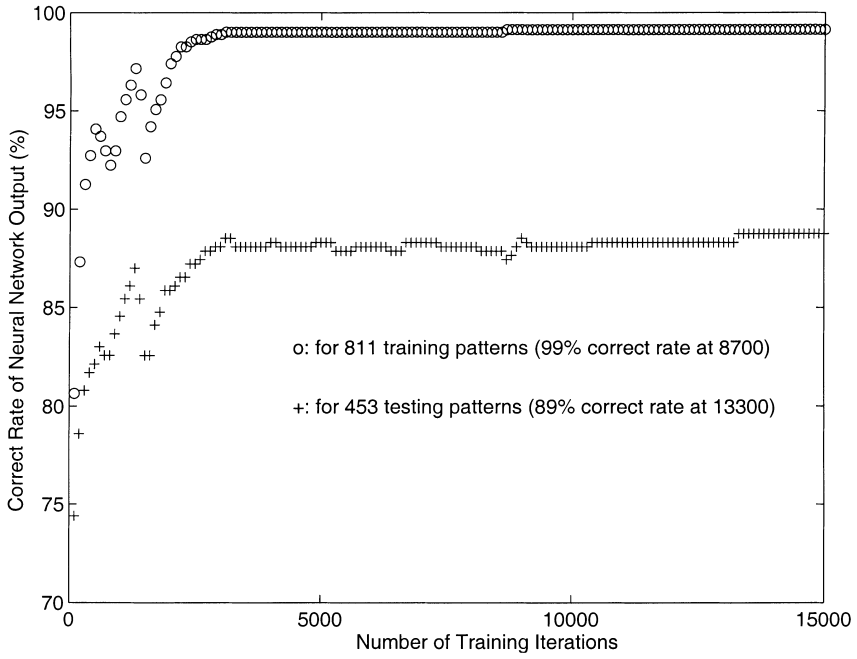

Figure 7
Training and test results of trained neural network (signals versus noise) with adaptive-1 training set. Output of the trained neural network now converges to 99% correct rate for the training data set and 89% for the testing data set.

the unlearned patterns correctly. The retrained neural network was tested by using the same testing data set as in the previous step. The correct rate for the testing data set increased from 77% to 89%. This increase was a significant improvement for classification. This improvement in classification with the adaptive-1 training data set does not indicate that better performance can be achieved with less information (fewer training patterns). In contrast, the proposed multi-step adaptive training process uses all of the information more efficiently.

Figure 7 shows that the adaptive-1 training data set still contains confused output. The next adaptive step is to delete the confused samples in both off-diagonal groups, N_{21} and N_{12}, from the adaptive-1 training data set. The group N_{12} is deleted in this step because the contaminating effect of the initial noise data set is assumed to have been minimized, and thus those small number of patterns is outliers of the signal class. The number of training data is reduced from 811 to 804. This reduced data set is called "adaptive-2" training data set. The neural network is retrained with the adaptive-2 training data set and tested with the same testing data set. The correct rate for the training data set increased to 100%, as shown in Figure 8. The correct rate for the same testing data set, however, is the same as in the previous adaptive

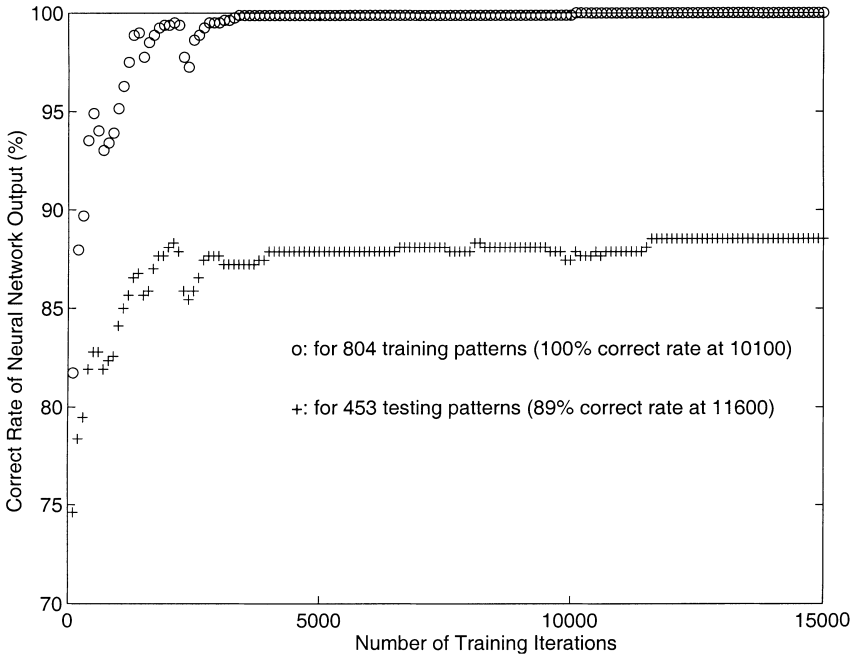

Figure 8
Training and test results of the trained neural network (signals versus noise) with adaptive-2 training set. Output of the trained neural network now converges to 100% correct rate for the training data set and 89% for the testing data set.

step, adaptive-1. This means that the second adaptive step has only a minor impact on the training results.

For stages 2 and 3 of initial phase identification (T and P versus S, and T versus P), a standard training procedure is used because all selected training patterns derive from the "ground-truth" signal database.

After training all three stages of neural networks, three sets of new weights of neural networks for initial phase identification were generated for station STKA. The new weights were applied to 130 days of data of station STKA in the analyst reviewed bulletin. This is the same data for which the performance of default weights were evaluated in Table 1. The initial wave type confusion matrix of the new output is shown in Table 3.

A comparison of the matrixes in Table 1 and 3 shows that a significant improvement has been obtained by the retrained neural networks. The "correct rate" of the output of the newly trained neural network compared to the default neural network has increased from 25.6% to 81.7%. The "N-phase rate" has decreased from 22.8% to 14.8%. While the number of T-type phases confused as P-type phases has been reduced from 1381 to 50, the number of P-type phases confused as T-type

Table 3

Confusion matrix of initial phase classification using new weights of neural networks with adaptive training set (1996/07/19–1996/11/25). Each row in the table is the result of the automatic system, and each column is the final result confirmed by analysts. Off-diagonal elements are misclassification numbers

		Results by analyst			Sum
		T	*P*	*S*	
Results by system	*T*	2236	6	1	2243
	P	50	8	0	58
	S	37	1	8	46
	N	400	3	5	408
	Sum	2723	18	14	2755

phases has increased marginally from 3 to 6. That is, the major decrease in confused *T*-type phases has been achieved at the cost of a small increase in confused *P*-type phases.

In summary, the "Adaptive Training Approach" has efficiently achieved the goal of updating default neural networks for initial wave-type classification with little human effort in constructing ground-truth databases.

5. Validation by the Ground-truth Noise Database

The neural networks that were retrained by the proposed "Adaptive Training Approach" outperform the default weights of neural networks for initial phase identification. This section will further validate that this approach performs against an analyst-reviewed ground-truth noise database constructed by analysts.

At the Center for Monitoring Research, SAIC, a ground-truth noise database for station STKA was constructed for validating the proposed "Adaptive Training Approach." When constructing the ground-truth noise database, the objective of the analyses was to classify automatic system detections as "noise" or "not-noise." To minimize ambiguity in noise selection, detections that had some "not-noise" characteristics were considered as being "not-noise," and therefore were not included in the noise database, even though the detections would not have passed a "real signal" threshold for inclusion in the final analyst reviewed bulletin. Numerous detections classified as "noise" by the automatic system were in fact considered to be "not-noise" of one variety or another. Other detections that were classified as "not-noise" by the automatic system were judged to be noise, and were reclassified as such during analysis. The noise detections included activity judged to be spikes, detections with little apparent distinction from preceding background in either amplitude or period content, and detections with very low vertical/horizontal coherency. These measurements were analyzed across at least three filter bands (0.5–2.0, 1.0–2.5 or 1.5–

3.0, and 3.0–6.0 Hz) that are commonly used to differentiate signal activity from noise during routine reviewing analysis. For station STKA, 898 noise phases were identified by the analysts after reviewing the waveform data of a five-day period during March 19–22, and March 27, 1997.

From this ground-truth noise database and the analyst reviewed bulletin, a training data set for the stage signals (*TPS*) versus noise (*N*) was constructed by random selection from the ground-truth databases. The number of training patterns and the ratio of signal detections to noise phases in the training set were selected intentionally to be about the same as those of the training data set that were automatically selected using the adaptive approach. The training set consists of 829 patterns, and the testing set consists of 426 patterns. The neural network for classification of signals and noise was trained with the ground-truth training data set. Figure 9 shows correct rates of output versus the number of training iterations for the neural network, which was trained by the ground-truth databases. For the given training data set and testing data set, the trained neural network converges to 95% and 84%, respectively, which are worse than the correct rates of the adaptively trained neural network.

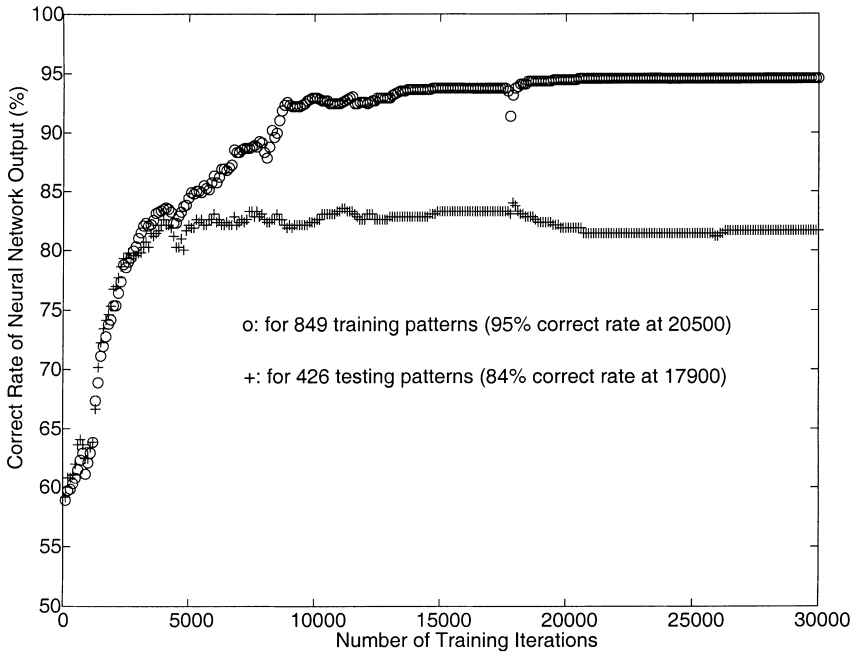

Figure 9
Training and test results of trained neural network (signals versus noise) with ground-truth training set. Output of the trained neural network converges to 95% correct rate for the training data set and 84% for the testing data set.

Using the new weights of the neural network trained by the ground-truth data set, the same 130 days of data of STKA were tested again. The initial phase confusion matrix of the new output is listed in Table 4. Combined with Tables 1, 3, and 4, Table 5 gives a summary of the performance for different weights of neural networks. In Table 5, the Default column represents the performance of the default neural networks, New-1 represents the performance of the neural networks trained by the adaptive training approach, and New-2 represents the performance of the neural networks trained by the ground-truth training set. From the table we can see that the performance of initial phase identification is similar for both sets of the new weight of neural networks. However, for the output of the New-2 neural networks, more seismic phases were incorrectly identified as noise phases than for the New-1 neural networks. There are two possible explanations to these results. Firstly, the ground-truth noise database was selected from only a few days, while the adaptive training approach randomly selected training patterns over a considerably longer time period. The latter would better reflect the seasonal variation of noise detections. Secondly, the consistency with which human beings analyze noisy data is limited by analyst skills and experience.

To further illustrate the effect of the Adaptive Training Approach, the Mahalanobis distances (DUDA and HART, 1973) between the four wave types for

Table 4

Confusion matrix of initial phase classification using new weights of neural networks with ground-truth training set (1996/07/19–1996/11/25). Each row in the table is the result of the automatic system, and each column is the final result confirmed by analysts. Off-diagonal elements are misclassification numbers

		Results by analyst			Sum
		T	*P*	*S*	
Results by system	*T*	2214	5	1	2220
	P	42	7	0	49
	S	22	0	3	25
	N	445	6	10	461
	Sum	2723	18	14	2755

Table 5

Summary of testing using different NNET-weights for STKA. The 'Default' columns represent the performance of the initial default neural networks, 'New-1' and 'New-2' represent the performance of the neural networks trained by the adaptive training approach, and by the 'ground-truth' data set, respectively

Number of phases	Correct rate (%)			*N*-phase rate (%)		
	Default	New-1	New-2	Default	New-1	New-2
2755	25.6	81.7	80.7	22.8	14.8	16.7

Table 6

Mahalanobis distances between four wave types. The final noise data set selected using the adaptive approach gives better distinction, i.e., longer distance, with signals

	P	*S*	Initial noise data set	Final noise data set	Analyst-selected noise data set
T	4.2932	11.5904	4.6344	6.1566	5.4520
P		9.1040	4.9523	6.2631	5.5160
S			2.6378	2.6539	2.3352
Signals (*T*, *P*, *S*)			2.5044	3.5499	2.9467

each training set are listed in Table 6. The Mahalanobis distance between two *N*-dimension populations is defined as follows:

$$MD = \sum_{j=1}^{N} \frac{(\mu_{j1} - \mu_{j2})^2}{\sigma_{j1}^2 + \sigma_{j2}^2} \quad .$$

It is a measure of the statistical distance between two classes based on their normal probability densities. In Table 6, the number in each cell represents Mahalanobis distance between the wave types in the corresponding row and column. Column 3 represents the Mahalanobis distances between signal wave types and the initial noise data set, which was automatically selected before training neural networks. Column 4 represents the Mahalanobis distances between signal wave types and the final noise data set, which was adaptive selected during the training process. Column 5 represents the Mahalanobis distances between the noise data selected by analysts and signal wave types. A comparison of column 5 with columns 3 and 4 indicates that the initial noise training data set has a closer distance to the signals than that of the analyst-selected noise data set, and the final noise data set has the further distance than that of the analyst-selected noise data set. This geometrical presentation demonstrates the adaptive characteristic of the proposed training approach.

6. Summary

The neural network applications developed for IMS stations have the ability to automatically identify for high-dimensional input data. The adaptive learning ability of neural networks makes retraining possible and easy for continuous operational systems.

The selection of training patterns is a key factor for the successful application of neural networks. The training of neural networks must accommodate the imperfect knowledge of the noise because no noise detections have been reviewed by analysts in the routine operation. Compared to seismic wave types (Teleseism, Regional *P*, and Regional *S*), the selection of a noise training set is considerably more difficult and

requires considerable analyst effort. An adaptive training approach to automatically select training data sets has therefore been proposed in this paper. This approach uses the adaptive learning ability of neural networks and information stored in the automatic operational database.

The neural networks for initial wave-type classification have been trained using the proposed approach for station STKA, and thus specific neural network weights have been generated. Testing result of the new weights of the retrained neural networks shows significant improvements with the "correct rate" increasing from 25.6% to 81.7%.

The proposed "Adaptive Training Approach" has been validated by the ground-truth noise database, which was constructed manually by analysts. Comparisons of the performance of phase identification and the statistical distribution of training patterns demonstrate that the proposed approach is efficient and reliable.

Acknowledgements

I am indebted to Hans Israelsson, Robert G. North, Keith Mclaughlin, and Chris Ferraro for their remarkable effort to enhance the manuscript of this paper. I especially thank Michael Clark and Richard A. Reed for their work in constructing the ground-truth noise database used in this work. I am also grateful to Tom Bache, Greg Beall, Roger Bowman, Rick Jenkins, Tom Sereno, and Henry Swanger for their invaluable assistance and suggestions. Dr. Zontan A. Der and two anonymous reviewers made valuable suggestions to improve this article. This work was supported by the U. S. Department of Defense, Defense Threat Reduction Agency (Contract Number DTRA-99-C-0025).

References

Anant, K. S. and Dowla, F. U. (1997), *Waveform Transform Methods for Phase Identification in Three-component Seismograms*, Bull. Seismol. Soc. Am. *87*, 1598–1612.

Bache, T. C., Bratt, S. R., Wang, J., Fung, R. M., Kobryn, C., and Given, J. W. (1990), *The Intelligent Monitoring System*, Bull. Seismol. Soc. Am. *80*, 1833–1851.

Cichowicz, A. (1993), *An Automatic S-phase Picker*, Bull. Seismol. Soc. Am. *81*, 180–189.

Duda, R. O. and Hart, P. E. *Pattern Recognition and Classification*, (John Wiley, New York, 1973) 482 pp.

Jurkevics, A. (1988), *Polarization Analysis of Three-component Array Data*, Bull. Seismol. Soc. Am. *78*, 1725–1743.

Roberts, R. G., Christoffersson, A., and Cassidy, F. (1989), *Real-time Event Detection, Phase Identification and Source Location Estimation Using Single-station Three-component Seismic Data*, Geophys. J. *97*, 471–480.

Rumelhart, D. E., McClelland, J. L., and the PDP Research Group (1986), *Learning Representations by Back-propagating Errors*, Nature *332*, 533–536.

Sereno, T. and Patnaik, G. (1993), *Initial Wave-type Identification with Neural Networks and its Contribution to Automated Processing in IMS Version 3.0*, Technical Report, SAIC-93/1219.

SUTEAU-HENSON, A, (1991), *Three-component Analysis of Regional Phases at NORESS and ARCESS: Polarization and Phase Identification*, Bull. Seismol. Soc. Am. *81*, 2419–2440.

WANG, J. and TENG, T. L. (1995), *Artificial Neural Network-based Seismic Detector*, Bull. Seismol. Soc. Am. *85*, 308–319.

WANG, J. and TENG, T. L. (1997), *Identification and Picking of S Phase using an Artificial Neural Network*, Bull. Seismol. Soc. Am. *87*, 1140–1149.

ZURADA, J. M. *Introduction to Artificial Neural Systems* (West Publishing Company, St. Paul, 1992) pp. 163–250.

(Received May 20, 1999, revised May 15, 2000, accepted May 29, 2000)